Theoret. chim. Acta (Berl.) 11, 8—25 (1968)

Electronic Structure of the Permanganate Ion

J. P. DAHL and H. JOHANSEN
Department of Physical Chemistry, The University of Copenhagen, Denmark

Received January 22, 1968

The electronic structure of the permanganate ion has been investigated, using a semiquantitative LCAO MO method without empirical parameters. The atomic orbital basis set for the central ion has been varied systematically, and the effect of symmetric changes of bond distances has also been examined. In addition, calculations have been performed in which the regions around the ligands have been made more attractive for electrons, to simulate the presence of cations in solution and in the crystalline state. The electronic absorption spectrum of MnO_4^- has been tentatively assigned, on the basis of predicted band shapes and transition energies.

Die Elektronenstruktur des Permanganations wurde mit einer halbquantitativen LCAO-MO Methode ohne empirische Parameter behandelt. Die Zustandsfunktionen des Zentralatoms wurden variiert und der Einfluß symmetrische Änderungen der Bindungsabstände untersucht. Um die Gegenwart von Kationen in Lösung und im Kristall zu simulieren, wurden daneben auch Rechnungen durchgeführt, bei denen einer stärkeren Elektronenanziehung durch die Liganden Rechnung getragen wird. Ferner wurde versucht, das Absorptionsspektrum von MnO_4^- auf Grund der vorausgesagten Bandenform und Übergangsenergien zu deuten.

La structure électronique de l'ion permanganate est étudiée à l'aide d'une méthode LCAO MO semi-quantitative sans paramètres empiriques. La base d'orbitales atomiques pour l'ion central a été systématiquement variée et l'effet de changements symétriques des longueurs de liaison a été aussi examiné. Pour simuler la présence des cations dans la solution et dans le cristal on a fait des calculs dans lesquels la région autour des ligands était rendue plus attractive pour les électrons. Le spectre d'absorption de MnO_4^- est interprété à l'aide des prédictions sur les formes des bandes et les énergies de transition.

1. Introduction

A number of molecular orbital calculations have been performed on transition metal complexes during the last few years. Most of these calculations make use of empirical parameters, derived from experimental data, referring either to the complexes themselves or to the ions from which the complexes are built. Since, however, the atomic orbitals of the free ions differ very much in shape and radial extension, the number of independent parameters is so large, that it is impossible to adhere to the important principle, that the number of experimental quantities used to fix the parameters should considerably exceed the number of parameters itself. Due to this fact, it is very difficult to estimate the amount of information content present in these calculations.

Now, it is not only in the selection of parameters that one must make a choice in a parameterized molecular orbital theory. As in any theory, in which at least some of the molecular integrals are actually evaluated, a decision must be made as to the radial form of the atomic orbitals used in the numerical work. The outcome of a calculation is, therefore, a presumably complicated function of parameter and atomic orbital choice. An understanding of the nature of this function should enable one to judge the validity of a prediction made by a parameterized

theory. A prediction which is fairly stable towards changes in parameter and atomic orbital choice would, in general, be considered more probable than one which is very sensitive to such changes.

In a recent review article [8] it was suggested that it might be possible to construct semiquantitative theories with an information content comparable to that of the parameterized theories. As defined here a semiquantitative theory operates without empirical parameters, but with a certain set of numerical approximations. Such a theory was presented in [8] and applied to the permanganate ion, MnO_4^-. No attempt was, however, made to vary the atomic orbitals involved.

In the present article we report a series of molecular orbital calculations for MnO_4^-, in the same semiquantitative scheme as was used in [8]. The atomic orbital basis set for the central ion has been varied systematically, and the effect of symmetric changes of bond distances has also been examined. In addition, we have performed calculations in which the regions around the ligands have been made more attractive for electrons, to simulate the presence of cations in solution and in the crystalline state.

The results from our calculations show that there are a number of features that are fairly insensitive to changes in the input conditions, but there are also features which are not. We believe that a good qualitative understanding of the electronic structure of MnO_4^- may be obtained through a consideration of our results, and that more questions can now be answered than before. But the results also demonstrate that it is fallacious to demand that theories of the present type, and also parameterized theories should be able to give quantitatively correct answers at this stage.

2. Description of Method

2.1. Core and Valence Orbitals

The method employed in the present set of calculations has been thoroughly described and discussed in [8], and so we shall confine ourselves to a brief outline here.

The molecular orbitals (MO's) of the complex are divided into core orbitals and valence orbitals. The core orbitals include the ligand 1*s* orbitals and the 1*s*, 2*s*, 2*p*, 3*s*, and 3*p* orbitals of the central metal ion; these orbitals are all assumed to be the same as in the free ions. The valence MO's, denoted φ_i, are constructed as linear combinations of atomic orbitals, LCAO's:

$$\varphi_i = \sum_{r=1}^{m} a_{ri}\chi_r \tag{1}$$

assuming m atomic orbitals (AO's), denoted χ_r. The AO's are of the types 3*d*, 4*s*, and 4*p* for the metal ion, and of the types 2*s* and 2*p* for the ligands. In an LCAO MO calculation one determines the coefficients a_{ri} of Eq. (1) for a given radial dependence of each AO. By allowing the radial functions of the χ_r's to vary by performing several LCAO MO calculations, one may gain information as to which radial functions are the best to use. The same kind of information may, of course, be obtained by introducing several AO's of the same symmetry in (1). This procedure, which would be the natural one to follow in a completely quantitative investigation, is, however, not practical within the set of approximations used in the present work.

2.2. Orthogonal Atomic Orbitals

It is convenient to replace the AO's χ_r with a set of orthonormal orbitals λ_r, following one of the methods suggested in an article by Löwdin [12]: The valence AO's are divided into two groups, group 1 consisting of the metal $3d$ orbitals and the ligand $2s$ and $2p$ orbitals, and group 2 containing the metal $4s$ and $4p$ orbitals. Within group 1 the AO's, $\chi_1, \chi_2, \ldots, \chi_p$ are orthogonalized to each other, by use of Löwdin's method of symmetrical orthogonalization [12]. The AO's of group 2, $\chi_{p+1}, \chi_{p+2}, \ldots, \chi_m$ which are already orthogonal to each other, are then orthogonalized to the orbitals of group 1, by use of the Schmidt method.

Expressed in terms of the orthonormal orbitals defined in this way, Eq. (1) becomes:

$$\varphi_i = \sum_{r=1}^{m} C_{ri} \lambda_r \tag{2}$$

and the MO coefficients given later in this article all refer to Eq. (2).

2.3. Self Consistent Field Equations and Integral Approximations

The ground state of the permanganate ion is a totally symmetric singlet state. In the Hartree-Fock model we represent it by a single Slater determinant:

$$\Psi = |\dot{\varphi}_1^{\text{core}} \bar{\varphi}_1^{\text{core}} \ldots \dot{\varphi}_q^{\text{core}} \bar{\varphi}_q^{\text{core}} \dot{\varphi}_1 \bar{\varphi}_1 \ldots \dot{\varphi}_n \bar{\varphi}_n| \tag{3}$$

with φ_j^{core} and φ_i standing for core and valence MO's respectively. The + and − refer to alpha and beta spin functions in the usual way.

The core orbitals, as defined in Section 2.1, are to a good approximation orthogonal to each other, and the "strong orthogonality condition":

$$\int \varphi_i(1)\, \varphi_j^{\text{core}}(1)\, d\tau_1 = 0 \quad \textit{for all} \quad (\varphi_i, \varphi_j^{\text{core}}) \textit{ pairs} \tag{4}$$

is also reasonably well fulfilled. It is then expedient to introduce the one-electron core operator:

$$H^{\text{core}}(1) = T(1) + \sum_g V_g(1) \tag{5a}$$

$$V_g(1) = -\frac{Z_g e^2}{r_{1g}} + \sum_{j \text{ on } g} (2J_j^{\text{core}} - K_j^{\text{core}}) \tag{5b}$$

where g numbers the various nuclei, with charges $Z_g e$. $T(1)$ is the kinetic energy operator, and J_j^{core} and K_j^{core} are the usual Coulomb and exchange operators:

$$J_j^{\text{core}}\, \varphi(1) = \int \frac{e^2}{r_{12}} \varphi_j^{\text{core}}(2)\, \varphi_j^{\text{core}}(2)\, d\tau_2 \cdot \varphi(1) \tag{6a}$$

$$K_j^{\text{core}}\, \varphi(1) = \int \frac{e^2}{r_{12}} \varphi_j^{\text{core}}(2)\, \varphi(2)\, d\tau_2 \cdot \varphi_j^{\text{core}}(1)\,. \tag{6b}$$

Application of Roothaan's method [22] then leads to the following set of equations [8]:

$$\sum_{s=1}^{m} \left\{ (r|H^{\text{core}}|s) + \sum_{t,u=1}^{m} P_{t,u} \left([rs|tu] - \frac{1}{2} [ru|ts] \right) \right\} C_{si} = \varepsilon_i \sum_{s=1}^{m} (\delta_{rs} + S_{rs}) C_{si} \tag{7}$$

with $r = 1, 2, \ldots, m$, and

$$(r|H^{\text{core}}|s) = \int \lambda_r^{(1)}\, H^{\text{core}}(1)\, \lambda_s(1)\, d\tau_1 \tag{8a}$$

$$[rs|tu] = \iint \lambda_r(1)\, \lambda_s(1) \frac{e^2}{r_{12}} \lambda_t(2)\, \lambda_u(2)\, d\tau_1\, d\tau_2\,. \tag{8b}$$

$P_{t,u}$ is an element of the charge and bond order matrix:

$$P_{t,u} = 2 \sum_{j=1}^{n} C_{tj} C_{uj} . \tag{9}$$

A number of semiquantitative features are now introduced to facilitate the evaluation of the integrals in Eq. (7). First, the quantities S_{rs} from the overlap integrals $\delta_{rs} + S_{rs}$ between group 1 AO's are assumed to be so small, that second and higher order terms in these quantities may be neglected. As shown by Löwdin [12], this leads to the relations

$$\lambda_r = \chi_r - \frac{1}{2} \sum_{s=1}^{p} S_{sr} \chi_s, \quad (r = 1, \ldots, p) . \tag{10}$$

Furthermore, we neglect products of the type $S_{rs} S_{tu}$ for $r, s, t \leqq p$ and $u > p$, so that

$$\lambda_r = \left(1 - \sum_{s=1}^{p} S_{sr}^2\right)^{-1/2} \left(\chi_r - \sum_{s=1}^{p} S_{sr} \chi_s\right), \quad (r = p+1, \ldots, m) . \tag{11}$$

After the substitution of Eqs. (10) and (11) into Eq. (7), the problem is to evaluate integrals of the types (8). In the evaluation of most of these integrals we adopt the following approximations:

$$\chi_r(1)\, \chi_s(1) = \tfrac{1}{2} S_{rs} (\chi_r(1)\, \chi_r(1) + \chi_s(1)\, \chi_s(1)) , \quad (r, s \leqq p) \tag{12a}$$

$$\chi_r(1)\, \chi_s(1) = S_{rs} \chi_r(1)\, \chi_r(1) \quad (r \leqq p,\ s > p) \tag{12b}$$

which may be looked upon as special cases of a formula given by Löwdin [11]:

$$\chi_r(1)\, \chi_s(1) = \alpha\, \chi_r(1)\, \chi_r(1) + \beta\, \chi_s(1)\, \chi_s(1) . \tag{13}$$

With $\alpha + \beta = S_{rs}$, the total charge of the distribution $\chi_r \chi_s$ is preserved by the approximation. By adopting different values for (α, β), as in (12), an attempt is made also to represent the dipole moment of $\chi_r \chi_s$ correctly. Eq. (12a) was first presented by Mulliken [13] on integral form.

The approximations (12) are not, in our scheme, used in the evaluation of integrals containing the kinetic energy operator, and for integrals involving the core operator they are only used when more than two centers are involved. In the remaining integrals the original charge distributions are retained.

With the present set of approximations the expressions for the integrals between the orthogonalized orbitals are considerably reduced. A further simplification is, however, introduced by considering all AO's as s-like in their angular dependence, except in evaluating overlap integrals and one- and two-center integrals arising from H^{core}. Our scheme has therefore much in common with the complete neglect of differential overlap (CNDO) method by Pople *et al.* [18], but instead of introducing parameters like these authors, we prefer to calculate all integrals exactly, using Corbató and Switendick's DIATOM programs [4]. As mentioned in the introduction, the number of independent parameters is so large in our case, that they cannot be determined from experimental results on MnO_4^-, and no ab initio calculation exists with which we can compare.

The approximations behind the present method have been thoroughly discussed in [8] and [6], to which the reader is referred for further discussion.

3. Radial Functions

This Section contains a specification of the radial functions which have been considered in our calculations. The radial functions for oxygen have not been varied, but we have, as mentioned earlier, performed calculations with a number of different manganese valence AO's.

Each radial function $R_{nl}(r)$ is represented by a linear combination of Slater-type orbitals (STO's):

$$R_{nl}(r) = \sum_{j=1}^{\nu(nl)} C_j R(n_j, \zeta_j) \tag{14}$$

with a single STO being of the form

$$R(n_j, \zeta_j) = \left[\frac{(2\zeta_j)^{2n_j+1}}{(2n_j)!}\right]^{1/2} r^{n_j-1} e^{-\zeta_j r}. \tag{15}$$

The individual STO's as well as the radial functions R_{nl} are normalized according to the relation:

$$\int_0^\infty R^2 r^2 \, dr = 1. \tag{16}$$

The oxygen AO's have been taken from Clementi and Raimondi's determination of minimal basis set STO's [3]. In the notation of Eq. (14) we have:

$$R_{1s}(r) = R(1, 7.6579)$$
$$R_{2s}(r) = -0.2371\, R(1, 7.6579) + 1.0277\, R(2, 2.2458)$$
$$R_{2p}(r) = R(2, 2.2266)$$

R_{2s} appears as a STO with $n=2$ and $\zeta = 2.2458$, which has been Schmidt orthogonalized to the $1s$ orbital

Table 1. *Core orbitals for* Mn

	n_j	ζ_j	C_j
$1s$	1	24.385	1.0000
$2s$	1	24.385	−0.3653
	2	9.325	1.0646
$3s$	1	24.385	0.1436
	2	9.325	−0.4835
	3	4.27	1.0985
$2p$	2	10.15	1.0000
$3p$	2	10.15	−0.3139
	3	3.955	1.0482

The manganese orbitals have been determined from the papers of Richardson *et al.* [20, 21]. Table 1 gives the fixed Mn core orbitals, used in all calculations, and the various $3d$, $4s$, and $4p$ orbitals used are listed in Tables 2–4. These valence AO's are all orthogonal to the core orbitals of Table 1.

The $3d$ orbitals of Table 2 denoted d^7, d^6, ..., d^2 have been determined from the configurations (Ar) $(3d)^7$, (Ar) $(3d)^6$, ..., (Ar) $(3d)^2$ respectively [20], with (Ar) standing for the closed argon core $(1s)^2$ $(2s)^2$ $(2p)^6$ $(3s)^2$ $(3p)^6$. The $3d$ orbitals are all of the "double zeta" type, being linear combinations of two STO's. Ortho-

Table 2. Mn 3*d orbitals*

Configuration	n_j	ζ_j	C_j
d^7	3	5.15	0.514
	3	1.70	0.693
d^6	3	5.15	0.532
	3	1.90	0.649
d^5	3	5.15	0.547
	3	2.10	0.605
d^4	3	5.15	0.565
	3	2.30	0.562
d^3	3	5.15	0.585
	3	2.50	0.519
d^2	3	5.15	0.605
	3	2.70	0.479

Table 3. Mn 4*s orbitals*

Configuration	n_j	ζ_j	C_j
$4s(d^6s^2)$	1	24.385	−0.0024
	2	9.325	0.0081
	3	4.270	−0.0193
	4	0.650	1.0002
$4s(d^5s^2)$	1	24.385	−0.0211
	2	9.325	0.0720
	3	4.270	−0.1794
	4	1.350	1.0133
$4s(d^4s^1)$	1	24.385	−0.0480
	2	9.325	0.1651
	3	4.270	−0.4338
	4	1.940	1.0754

Table 4. Mn 4*p orbitals*

Configuration	n_j	ζ_j	C_j
$4p(d^6p^2)$	2	10.15	0.002861
	3	3.955	−0.009868
	4	0.51	1.000044
$4p(d^5p^2)$	2	10.15	0.029676
	3	3.955	−0.10508
	4	1.06	1.00502
$4p(d^4p^1)$	2	10.15	0.07384
	3	3.955	−0.27012
	4	1.52	1.03270

gonality requirements would not exclude simple STO's but it is known from previous investigations [7, 20] that a single STO cannot represent an atomic 3*d* orbital with sufficient accuracy, neither in the internal nor the external region of an atom. This point has recently been thoroughly discussed by Brown and Fitzpatrik [2]. It may be noted that all *d* orbitals correspond to configurations with

empty 4*s* and 4*p* shells. This is due to the fact that the form of a 3*d* orbital is quite independent of the population of these outer shells, as first shown by Watson [23].

The notation for the 4*s* and 4*p* orbitals has also been chosen so as to indicate the configuration from which the orbitals have been determined. A 4*p* orbital may be considered as a STO with $n=4$, which has been Schmidt orthogonalized to the 2*p* and 3*p* orbitals of the core. Similarly, a 4*s* orbital may be considered as a STO with $n=4$, orthogonalized to the 1*s*, 2*s*, and 3*s* orbitals. Use has been made of this fact in constructing the 4*s* orbitals $4s(d^6s^2)$ and $4s(d^4s^1)$ in Table 3. 4*s* functions for the configurations (Ar) $(3d)^6$ $(4s)^2$ and (Ar) $(3d)^4$ $(4s)^1$ do not exist in the literature, and we have therefore constructed such functions by demanding that

$$\frac{\zeta_{4s}(d^6s^2)}{\zeta_{4p}(d^6p^2)} = \frac{\zeta_{4s}(d^5s^2)}{\zeta_{4p}(d^5p^2)} \tag{17}$$

for the $4s(d^5s^2)$ orbital, and

$$\frac{\zeta_{4s}(d^4s^1)}{\zeta_{4p}(d^4p^1)} = \frac{\zeta_{4s}(d^5s^2)}{\zeta_{4p}(d^5p^2)} \tag{18}$$

for the $4s(d^4s^1)$ orbital. These relations fix, by means of the orbital $4s(d^5s^2)$ and the three 4*p* orbitals of Table 4, the 4*s* STO's with $n=4$. Schmidt orthogonalization to the core functions then results in the orbitals of Table 3.

The orbitals of Tables 2, 3 and 4 are in the following considered as a set of possible valence AO's for Mn, from which the best AO's for an MO calculation are to be chosen. It is not claimed that the relations (17) and (18) furnish the best AO's for atomic states, rather they supply a set of 4*s* functions wich are convenient for our purpose.

4. Results and Discussion

The results from our calculations are presented in the following set of tables and figures. Unless otherwise specified the Mn–O distance has been taken as 1.629 Å, from the recent determination by Palenik [15]. This distance differs slightly from the value 1.59 Å used in the two permanganate calculations reported in reference [8].

4.1. Search for Best Atomic Orbitals

According to the variational principle, the best MO's are obtained by minimizing the total energy of the system considered. This principle leads directly to Roothaan's equations [22] for a fixed set of AO's, and also to the requirement that one should look for an optimal basis set of AO's in the sense, that such a set of AO's, in conjunction with Roothaan's equations, should result in a lower energy than any other basis set of the same size. In parameterized theories and semiquantitative theories like the present one, the variational principle is applied to an energy expression which is only approximately correct. Hence the results from a search for an optimal basis set must be interpreted with some caution. The same holds, of course, for the results from a search for optimal coefficients in the LCAO's through an application of Roothaan's equations. It is in harmony with this point of view to use AO's of a simple form and only to vary these on a coarse mesh.

The oxygen orbitals have not been varied here, because it is known from ab initio calculations on smaller molecules, that the optimal first row AO's to be used in ground state MO's differ only slightly from the best AO's for free atoms. (See, for instance, references [19, 17], and [1].) The differences are too small to be of significance in the present type of investigation. It would, however, be premature to conclude that the experience gained regarding the first row AO's can be transferred directly to the third row AO's of the types $3d$, $4s$, and $4p$. The factors governing the change of AO's during molecule formation operate together in a complicated way, as demonstrated by Coulson [5], and it is also known that the hydrogen $1s$ orbital changes drastically during molecule formation [19], and that $2p$ orbitals optimized for excited states may be very different from the free atom $2p$ orbitals [10].

We have, therefore, attempted to minimize the energy of the closed shell wave function (3) in order to determine the best AO's of the types $3d$, $4s$, and $4p$. The total energy, E_t may be written

$$E_t = E_{\text{core}} + E \tag{19}$$

where

$$E_{\text{core}} = \sum_{i=1}^{q} \left\{ \int \varphi_i^{\text{core}}(1) \left[T(1) - \sum_g \frac{Z_g e^2}{r_{1g}} \right] \varphi_i^{\text{core}}(1)\, d\tau_1 + \int \varphi_i^{\text{core}}(1)\, H^{\text{core}}(1)\, \varphi_i^{\text{core}}(1)\, d\tau_1 \right\} + \sum_{g>h} \frac{Z_g Z_h e^2}{r_{gh}} \tag{20}$$

and

$$E = \sum_{i=1}^{n} \{\varepsilon_i + \int \varphi_i(1)\, H^{\text{core}}(1)\, \varphi_i(1)\, d\tau_1\} \tag{21}$$

E_{core} depends only on the nature of the core, and is thus the same for all calculations in which the Mn–O distance is the same. The variation of E_t is therefore given by the variation of E, when the valence AO's alone are varied.

In Table 5 we give the energy E in atomic units (1.a.u. = 27.21 eV) for two different choices of $3d$ function, viz. $3d(d^7)$ and $3d(d^4)$. For each $3d$ orbital, calculations have been performed for all possible pairs of $4s$ and $4p$ orbitals that can be taken from Tables 3 and 4. It is seen that E, for both choices of $3d$ function, is a mini-

Table 5. *Variation of the energy E as function of* 4s *and* 4p *orbitals. Energies in atomic units (1a.u. = 27.21 eV)*

		$4s(d^6s^2)$	$4s(d^5s^2)$	$4s(d^4s^1)$
$3d(d^7)$	$4p(d^6p^2)$	−172.34	−173.79	−173.34
	$4p(d^5p^2)$	−175.38	−176.44	−175.80
	$4p(d^4p^1)$	−174.58	−175.54	−174.40
$3d(d^4)$	$4p(d^6p^2)$	−171.35	−172.94	−171.75
	$4p(d^5p^2)$	−174.34	−175.63	−174.67
	$4p(d^4p^1)$	−173.75	−174.81	−173.61

mum for the functions $4s(d^5s^2)$ and $4p(d^5p^2)$. For this reason we expect the best in situ $4s$ and $4p$ orbitals to be quite close to these functions. So far as the $4s$ orbital is concerned, the function is the same as in the free atom.

With the orbitals $4s(d^5s^2)$ and $4p(d^5p^2)$ a series of calculations have been performed, in which the $3d$ orbital has been varied. The resulting energies are

shown in Table 6. Shown is also, for each calculation, the population of the $3d$ shell. With reference to Eq. (9) this population is defined as $\sum_t P_{tt}$, where the sum over t is over the five $3d$ orbitals. It is seen from Table 6, that the energy E decreases as the $3d$ orbital expands, i. e. with increasing population of the $3d$ shell. There is, however, no indication of a minimum in E; indeed, E decreases almost linearly throughout the series of functions $3d(d^2), \ldots, 3d(d^7)$. It is, however, noted that the energy varies much less throughout Table 6 than throughout Table 5, and this makes it understandable that our approximations prevent the appearance of a minimum in Table 6. We may, however, take the results of that table to indicate, that there is a tendency for the $3d$ orbital to expand during molecule formation. We assume, therefore, that the best $3d$ orbitals are $3d(d^6)$ or $3d(d^7)$. This assumption leads to a $3d$ shell population close to five, which is very reasonable, since a free Mn atom contains five $3d$ electrons.

Table 6. *Variation of the energy E as function of the 3d orbital, with the 4s and 4p orbital fixed as* $4s(d^5s^2)$ *and* $4p(d^5p^2)$

$3d$ orbital	E (a.u.)	Population of $3d$ shell
$3d(d^7)$	−176.44	5.12
$3d(d^6)$	−176.15	4.65
$3d(d^5)$	−175.91	4.39
$3d(d^4)$	−175.63	4.18
$3d(d^3)$	−175.31	3.98
$3d(d^2)$	−175.02	3.80

The five $3d$ orbitals span the irreducible representations e and t_2 in a tetrahedral molecule, and there is therefore the possibility that different $3d$ orbitals should be used for these two representations. We have studied this possibility, but our results are quite insensitive to differences in the two orbitals. It is the choice for the t_2 orbital which determines the energy and the molecular orbital level diagram. Use of the $3d(d^7)$ orbital for t_2 and the $3d(d^5)$ orbital for e leads, for instance, to an energy $E = -176.43$ a.u., which is the same value as is obtained when the $3d(d^7)$ orbital is used for both representations. It is therefore not necessary, in our approximation, to work with two different radial functions for the $3d$ orbitals.

The conclusion of the present section is then, that one should use free atom AO's for the ligands. The Mn $4s$ and $4p$ orbitals should be taken as $4s(d^5s^2)$ and $4p(d^5p^2)$ and the orbitals $3d(d^7)$ or $3d(d^6)$ should be used as $3d$ orbitals, for both e and t_2 representations.

4.2. Molecular Orbitals as Functions of Metal AO's

The MO's of a tetrahedral molecule have symmetry designations a_1, e, t_1, and t_2, and they are in the LCAO approximation represented as linear combinations of symmetry adapted orbitals. The symmetry adapted orbitals are again linear combinations of atomic orbitals, in our case orthogonalized AO's. We refer to reference [8] for a full specification of the form of the symmetry adapted orbitals used in the present work.

In Table 7 we present the MO energies ε_i of Eq. (7), resulting from a set of calculations in which the Mn 3*d* radial function was kept fixed as $3d(d^7)$, and the 4*s* and 4*p* orbitals were varied, as in Table 5. The orbitals $2e$, $4t_2$, $3a_1$, and $5t_2$ are all empty, whereas the remaining ones are fully occupied with electrons. The MO energies are seen to be highly dependent on the 4*s* and 4*p* orbitals chosen, which is not too surprising. Of more interest, however, is the fact that also the order of the MO levels is quite sensitive to variations in the 4*s* and 4*p* orbitals. This is especially true for the order of the highest occupied orbitals, whereas the order of the empty orbitals is $2e < 4t_2 < 3a_1 < 5t_2$ in all cases, except in the calculation (2, 1) where $2e$ and $4t_2$ are approximately degenerate, and (3, 1) where the order of $2e$ and $4t_2$ is reversed. All in all Table 7 emphasizes the necessity of performing the search for optimal AO's, described in the preceding section.

Table 7. *MO energies in eV as functions of* Mn 4*s and* 4*p orbitals with the* 3*d orbital fixed as* $3d(d^7)$[a]

s, *p*	1, 1	1, 2	1, 3	2, 1	2, 2	2, 3	3, 1	3, 2	3, 3
a_1	8.377	3.928	6.361	10.828	3.955	9.339	12.682	7.312	14.742
	− 5.610	−10.098	− 6.282	−15.442	−17.840	−12.895	−11.396	−11.757	− 3.836
	−27.860	−31.189	−28.215	−34.926	−36.681	−32.043	−22.743	−27.534	−21.551
e	1.209	− 1.983	2.576	3.688	− 2.287	4.498	6.506	0.731	8.173
	−11.674	−15.522	−10.305	− 9.380	−15.162	− 8.830	− 7.262	−12.203	− 5.049
t_2	14.630	10.073	14.650	16.811	11.212	17.146	18.358	13.009	19.438
	3.063	2.150	5.185	3.683	1.691	6.974	3.928	3.427	9.807
	− 7.870	−12.655	− 9.767	− 6.853	−13.354	− 8.487	− 5.662	−11.216	− 5.338
	−13.547	−24.858	−19.934	−11.853	−23.934	−17.450	−10.205	−22.513	−15.244
	−30.788	−36.385	−31.185	−29.125	−36.559	−29.715	−27.275	−34.332	−26.220
t_1	− 7.670	− 9.401	− 6.812	− 6.685	−11.576	− 6.583	− 5.454	− 9.077	− 2.656

[a] The 4*s* and 4*p* orbitals used are specified by pairs of numbers in the heading of the table, so that *i*, *k* stands for the *i*'th 4*s* orbital and the *k*'th 4*p* orbital, according to the orders $4s(d^6s^2)$,$4s(d^5s^2)$,$4s(d^4s^1)$ and $4p(d^6s^2)$, $4p(d^5p^2)$, $4p(d^4p^1)$.

Fig. 1 shows how the MO energies vary with the Mn 3*d* radial functions, with the 4*s* and 4*p* orbitals fixed as the "optimal" orbitals $4s(d^5s^2)$ and $4p(d^5p^2)$. It is seen that the locations of the important *e* orbitals are very dependent on the choice of the 3*d* radial function, but otherwise the order of the molecular orbitals is rather stable. On the basis of the arguments presented in Section 4.1 it is the first two columns in Fig. 1 which should represent the most likely molecular orbital level diagram for MnO_4^-.

In Tables 8 and 9 we list the coefficients of the MO's corresponding to columns 1 and 4 in Fig. 1. It is again clear that it is the *e* orbitals which are most sensitive to the form of the 3*d* radial function. A prominent feature of tables 8 and 9 is the fact that the orbitals 4*s* and 4*p* are strongly mixed into the occupied orbitals. For a further discussion of the MO coefficients we refer to ref. [8], where Table 8 also is presented, with the slight modification that the Mn–O distance is chosen as 1.59 Å instead of 1.629 Å, as used here.

4.3. Molecular Orbitals as Functions of Mn–O Distance

It is of considerable importance to know how an MO level diagram depends on bond distance, and we have therefore performed calculations in which the

Mn–O bond length has been varied, using the Mn orbitals $3d(d^7)$, $4s(d^5s^2)$, and $4p(d^5p^2)$. The results from these calculations are shown in Fig. 2. Calculations were performed for the Mn-distances 1.552 Å, 1.590 Å, 1.629 Å, 1.659 Å, and 1.689 Å. The first of these distances is the average value of the Mn–O distances given by Wyckoff [24], the second value was used by Oleari *et al.* [14] and in Ref. [8]. The value 1.629 Å was determined by Palenik [15] and has been used extensively in the present work. Finally, the value 1.659 Å is the Mn–O distance in MnO_4^{2-}, as determined by Palenik [16], and the value 1.689 Å is the extrapolated Mn–O distance in MnO_4^{3-}.

The MO energies are seen to be linear functions of the Mn–O distance, and apart from the crossing of the $1a_1$ and the $1t_2$ orbitals, the order of the MO's remains unchanged between 1.55 and 1.70 Å. The slopes of the different lines in

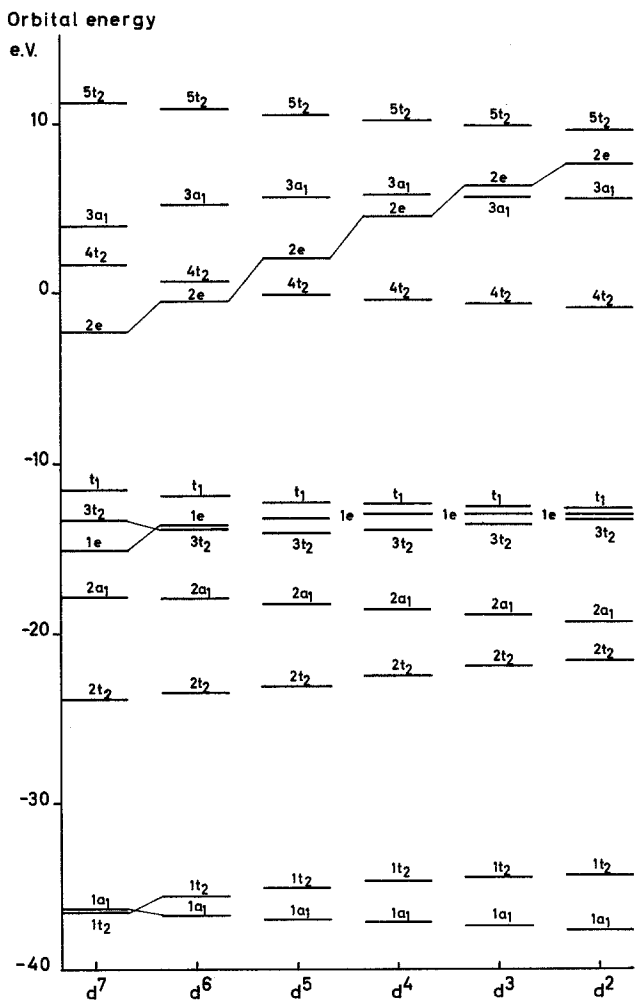

Fig. 1. MO level diagram as depending on the form of the Mn 3*d* radial function. The abscissa indicates the configuration from which the atomic 3*d* radial function has been derived (see Section 3)

Table 8. *Molecular orbitals for* MnO_4^-, *corresponding to the metal orbitals* $3d(d^7)$, $4s(d^5s^2)$, $4p(d^5p^2)$

Eigenvalues (eV)		Eigenvectors				
		s	σ_s	σ_p		
a_1	3.955	−0.3790	−0.1151	0.9182		
	−17.840	0.7125	0.5969	0.3689		
	−36.681	−0.5905	0.7941	−0.1442		
		d	π			
e	− 2.287	0.7208	−0.6932			
	−15.162	0.6932	0.7208			
		p	d	σ_p	σ_s	π
t_2	11.212	−0.3085	−0.5176	0.7777	0.0830	0.1587
	1.691	−0.6184	0.4461	−0.0143	−0.3806	0.5254
	−13.354	−0.1809	0.4028	0.3822	−0.2939	−0.7567
	−23.934	0.6273	0.4845	0.4975	0.0190	0.3519
	−36.559	−0.3140	0.3689	0.0377	0.8727	−0.0485
		π				
t_1	−11.576	1.0000				

Table 9. *Molecular orbitals for* MnO_4^-, *corresponding to the metal orbitals* $3d(d^4)$, $4s(d^5s^2)$, $4p(d^5p^2)$

Eigenvalues (eV)		Eigenvectors				
		s	σ_s	σ_p		
a_1	5.818	−0.3244	−0.1010	0.9405		
	−18.546	0.7150	0.6248	0.3137		
	−37.156	−0.6193	0.7742	−0.1305		
		d	π			
e	4.533	0.9744	−0.2248			
	−12.979	0.2248	0.9744			
		p	d	σ_p	σ_s	π
t_2	10.209	−0.3823	−0.3610	0.8338	−0.0273	0.1660
	− 0.378	−0.5605	0.4539	−0.1870	−0.3253	0.5823
	−13.903	−0.1495	0.6009	0.3149	−0.2750	−0.6647
	−22.466	0.5961	0.5003	0.4112	0.2028	0.4292
	−34.666	−0.4025	0.2287	−0.0396	0.8813	−0.0860
		π				
t_1	−12.368	1.0000				

Fig. 2 vary, however, considerably, and this is a point of great importance for the understanding of the electronic spectrum, as it will be emphasized in Section 4.5.

Fig. 2 may also partly answer the question, how accurate a structure analysis should be in order to provide a satisfactory geometry for use in MO calculations. An accuracy of ± 0.1 Å is apparently sufficient for theories like the present, in which one should not attach too much significance to the exact numbers, but only trust the qualitative aspects. But Fig. 2 also indicates that an accuracy of ± 0.01 Å might well be desirable in exact calculations to come.

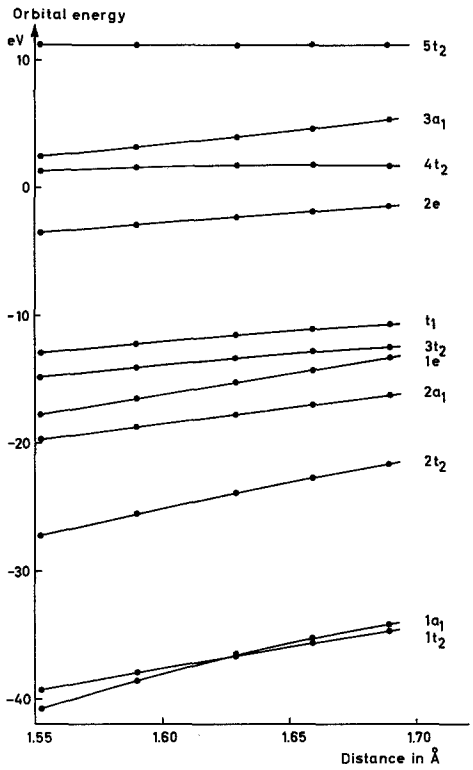

Fig. 2. MO level diagram as function of the Mn–O distance

4.4. *Variation of Ligand Potential*

The calculations mentioned so far all refer to an isolated MnO_4^- ion. In practice, however, the MnO_4^- ion is always embedded either in a crystal or in a solution, and it must be expected that nearby cations will create a potential, which is more attractive for electrons in the regions around the ligands than in the region around the Mn ion. As suggested in Ref. [8] this feature may be taken into account by subtracting a certain positive number, Δ^{core} from all integrals of the type $\int \chi_r(1)\, H^{\text{core}}(1)\, \chi_r(1)\, d\tau_1$ where χ_r is a non-orthogonalized ligand AO.

Fig. 3 shows the MO energies as function of Δ^{core}, corresponding to the Mn orbitals $3d(d^7)$, $4s(d^5s^2)$, and $4p(d^5p^2)$. The MO energies are seen to vary linearly with Δ^{core} over the range considered. Also the gap between the occupied and the empty orbitals (i.e. between t_1 and $2e$) increases with Δ^{core}, and this fact may be used, as in Ref. [8], to place the first transition energy correctly, i.e. Δ^{core} may be used as a semiempirical parameter. In this way one would, presumably, not only correct for some of the influences from the surroundings, but also for errors in the relative positions of metal and ligand orbitals on the energy scale. Such errors may occur because of the approximations of our model.

4.5. *Electronic Transition Energies*

The non-occupied MO's obtained by our calculations may be used to construct wave functions for excited states of the MnO_4^- ion, by transferring electrons

from filled to empty orbitals. The ground state wave function for MnO_4^- has symmetry $^1A_1$, and since the electric dipole vector transforms as T_2, all electric dipole allowed transitions are to excited states of symmetry $^1T_2$. One excited state of symmetry $^1T_2$ may be derived from each of the one-electron transitions

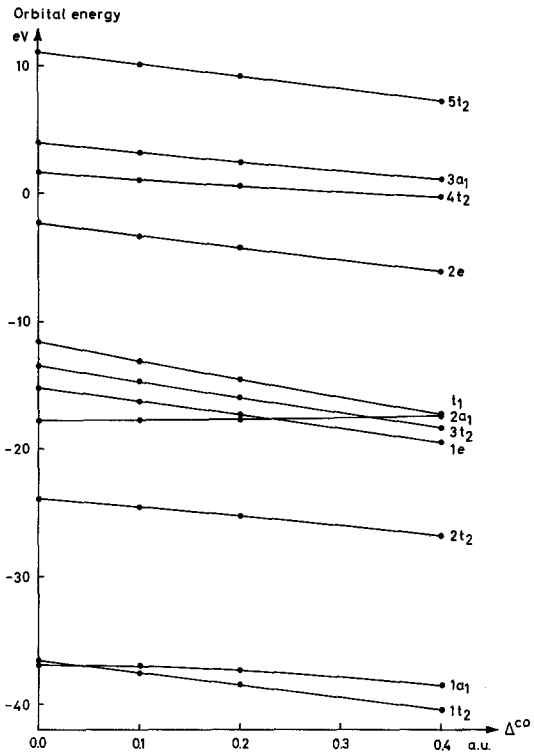

Fig. 3. MO level diagram as function of Δ^{core}

shown in Fig. 4. The transition energies $\Delta E_{i\to k}$ are in that figure shown as functions of the 3*d* radial function, and are defined as

$$\Delta E_{i\to k} = \varepsilon_k - \varepsilon_i - J_{ik} \tag{22}$$

where the transition $i\to k$ corresponds to the transfer of an electron from the occupied orbital φ_i to the empty orbital φ_k. J_{ik} is the usual Coulomb integral:

$$J_{ik} = \int \varphi_i(1)\,\varphi_i(1)\frac{e^2}{r_{12}}\varphi_k(2)\,\varphi_k(2)\,d\tau_1\,d\tau_2\,. \tag{23}$$

Eq. (22) is not the correct expression for the energy associated with $a^1A_1 \to {}^1T_2$ transition, but differs from it through important two-electron integrals [8], which serve to separate the various electronic states associated with the one-electron transition. These integrals are considerably smaller than J_{ik}, however, and will in general give a positive contribution to $\Delta E_{i\to k}$. Such integrals can not be evaluated with sufficient accuracy by a straightforward application of the CNDO approximation, and instead of evaluating them in a ZDO approximation we have left them out altogether. One further reason for doing so is supplied by the fact, evident from Fig. 4, that the calculated transition energies are extremely

sensitive to changes in the radial functions used, so that it is difficult to attach any quantitative meaning to the calculated transition energies. Still, Fig. 4 contains some useful information, when it is considered together with other aspects of the calculation.

According to Section 4.1, one should only attach significance to the results from the calculations, in which the $3d$ radial function has been taken as $3d(d^7)$ or

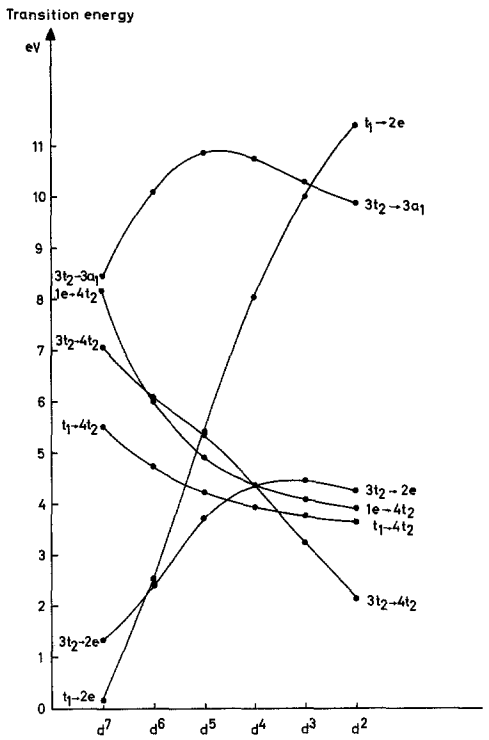

Fig. 4. Transition energies as functions of the Mn $3d$ radial function. Mn $4s$ and $4p$ functions are taken as $4s(d^5s^2)$ and $4p(d^5p^2)$

$3d(d^6)$, and we shall therefore in the following limit ourselves to these cases. The remaining part of Fig. 4 reminds of the necessity of looking for optimal AO's in an LCAO MO calculation.

5. Interpretation of the Electronic Absorption Spectrum

The electronic absorption spectrum of the MnO_4^- ion has been the subject-matter of much discussion. We refer to Ref. [8] for a comparison of the results from various theoretical investigations and add here only the information obtained through the present set of calculations.

The most complete absorption spectrum of MnO_4^- has been recorded by Holt and Ballhausen [9], who examined a solid solution of $KMnO_4$ in $KClO_4$ at liquid hydrogen and helium temperatures. Four band systems were observed and discussed:

The first band system has its maximum at about 20,000 cm^{-1} and shows a very complicated vibrational pattern. Holt and Ballhausen were able to conclude

that this band system represents a single electronic transition from the orbitally non-degenerate ground state to a threefold orbitally degenerate state.

The second band system covers the region from 25,000 cm^{-1} to 30,000 cm^{-1} and consists of seven peaks superimposed upon a strong background.

The third band system shows a very regular progression in 750 cm^{-1}, the maximum occurring at 33,000 cm^{-1}. Only a single electronic transition is involved.

The fourth band system has its maximum at 43,500 cm^{-1} and is completely featureless; it represents again a single electronic transition.

Holt and Ballhausen discussed the interpretation of this spectrum on the basis of the calculations presented in [8], but only a very tentative assignment was possible. With the present set of calculations we are, however, able to take one more step forward towards the understanding of this puzzling spectrum.

Table 10. *Molecular transition energies in eV, as functions of* Mn–O *distance R in* Å. Mn *radial functions are* $3d(d^7)$, $4s(d^5s^2)$, $4p(d^5p^2)$

Transition	R				
	1.552	1.590	1.629	1.659	1.689
$t_1 \rightarrow 2e$	0.01	0.00	0.18	0.22	0.57
$3t_2 \rightarrow 2e$	1.58	1.41	1.33	1.21	1.28
$t_1 \rightarrow 4t_2$	6.44	5.95	5.52	5.17	4.84
$3t_2 \rightarrow 4t_2$	8.18	7.61	7.05	6.65	6.28
$1e \rightarrow 4t_2$	10.27	9.21	8.16	7.43	6.67
$3t_2 \rightarrow 3a_1$	8.23	8.29	8.45	8.66	9.09

The one-electron transitions of Fig. 4 are in Table 10 presented as functions of the Mn–O separation, for the $3d$ radial function $3d(d^7)$. The fact that the first transition energy is almost zero is a consequence of the fact that we have desisted from using semiempirical parameters in our calculations. The transition energies would be pushed up by using, for instance, a non-zero value for Δ^{core}, as discussed in [8] and section 4.4, and also Eq. (22) is incomplete as mentioned in Section 4.5.

The important information in Table 10 is, that the transitions $t_1 \rightarrow 2e$, $3t_2 \rightarrow 2e$, and $3t_2 \rightarrow 3a_1$ allow the formation of excited states which are stable with respect to symmetric distortions, and with an Mn–O distance close to the one found in the ground state, whereas the transitions $t_1 \rightarrow 4t_2$, $3t_2 \rightarrow 4t_2$, and $1e \rightarrow 4t_2$ result in dissociative states. The first three transitions should therefore lead to absorption bands with a pronounced vibrational structure at low temperatures, whereas the last three transitions should result in broad, featureless bands. The half-widths of these bands may be estimated from Table 10 as follows.

The totally symmetric zero-point vibration is governed by the wave function

$$\psi_0(x) = \left(\frac{\alpha}{\pi}\right)^{1/4} e^{-\alpha x^2/2} \tag{24}$$

where x measures the magnitude of the totally symmetric displacement from the "equilibrium" position, and $\alpha = 4\pi^2 M \nu c/h$. To a good approximation M may be taken as the mass of the oxygen atom; ν is the totally symmetric vibration frequency in cm^{-1}, and h is Planck's constant. The half-width δ of the gaussian

function $|\psi_0(x)|^2$ is $[\ln 2/\alpha]^{1/2}$, and under the assumption that $\nu \approx 800\ \mathrm{cm}^{-1}$ [9], we find that $\delta \approx 0.043$ Å.

The half-widths of the bands associated with the transitions $t_1 \rightarrow 4t_2$, $3t_2 \rightarrow 4t_2$, and $1e \rightarrow 4t_2$ may then be estimated from Table 10 as the variations in the transition energies over a range of 0.06 Å, when the slight variation of the ground state energy over this range is neglected. We find for the three transitions mentioned the half-widths $3900\ \mathrm{cm}^{-1}$, $4700\ \mathrm{cm}^{-1}$, and $8800\ \mathrm{cm}^{-1}$, respectively.

From Fig. 4 it follows that our calculations predict two low lying absorption bands with pronounced vibrational structure. These bands arise from an interaction between the $t_1 \rightarrow 2e$ and $3t_2 \rightarrow 2e$ transitions. The interaction is strong, if $3d(d^6)$ is the optimal orbital, but if the optimal orbital is $3d(d^7)$ then the first of the transitions is mostly $t_1 \rightarrow 2e$, the second mostly $3t_2 \rightarrow 2e$. We associate the first and third band systems with these two transitions.

Fig. 4 indicates that the $3t_2 \rightarrow 3a_1$ transition occurs at too high energies to require consideration in the present context. We are then left with the transitions $t_1 \rightarrow 4t_2$, $3t_2 \rightarrow 4t_2$, and $1e \rightarrow 4t_2$ which should all lead to featureless bands. If $3d(d^7)$ is the optimal orbital then the three transitions should not mix heavily, and they should all lead to absorption at high energies. As in Ref. [8], we would in this case leave the second band system unexplained and associate the fourth band system with a transition which is mainly $t_1 \rightarrow 4t_2$.

If, however, the optimal orbital is $3d(d^6)$, then the most likely assignment would be the following: The first and third band systems correspond to mixtures of the $t_1 \rightarrow 2e$ and $3t_2 \rightarrow 2e$ transitions; the featureless background of the second band system corresponds to the $t_1 \rightarrow 4t_2$ transition, pushed down by configuration interaction, and the fourth band system corresponds to a heavy mixture of the $3t_2 \rightarrow 4t_2$ and $1e \rightarrow 4t_2$ transitions. The fine structure of the second band system remains unexplained by this assignment, but may be associated with an orbitally forbidden transition.

According to the measurements by Holt and Ballhausen [9] the half-widths of the second and third band systems are about $4000\ \mathrm{cm}^{-1}$ and $6500\ \mathrm{cm}^{1}$, and these findings would seem to support the second assignment above, corresponding to the $3d(d^6)$ orbital, when a comparison is made with the half-widths estimated from our calculations.

An important conclusion to be drawn from the present set of calculations is that the outcome from a calculation of transition energies is extremely sensitive to the radial functions chosen. This feature must of course hold for semiempirical as well as for semiquantitative models. It does not, however, mean that such models are worthless, since, as we have demonstrated in the present section, it is possible to arrive at a *probable* assignment of the electronic spectrum, but one should certainly be careful not to jump to conclusions from a single calculation.

6. Conclusion

The present set of calculations constitutes one of the most detailed theoretical investigations carried out so far for the MnO_4^- ion. It is hoped that it will be of qualitative use in further experimental examinations, until it becomes possible to perform an ab initio calculation for this ion.

Acknowledgment. It is a pleasure to thank Professor C. J. Ballhausen for his continued interest in this work, as manifested through numerous fruitful discussions. The Carlsberg Foundation is thanked for having placed a Friden 132 calculator at our disposal.

Literature

1. Allen, L. C.: Quantum theory of atoms, molecules, and the solid state. Editor P. O. Löwdin. New York: Academic Press 1966.
2. Brown, D. A., and N. J. Fitzpatrick: J. chem. Soc. (London) **1966** A, 941.
3. Clementi, E., and D. L. Raimondi: J. chem. Physics **38**, 2686 (1963).
4. Corbató, F. J., and A. C. Switendick: Methods in computational physics, B. Alder, S. Fernbach, and M. Rodenberg, eds. Vol. 2, p. 155. New York: Academic Press 1963.
5. Coulson, C. A.: Trans. Faraday Soc. **33**, 1479 (1937).
6. Dahl, J. P.: Acta chem. scand. **21**, 1244 (1967).
7. —, and C. J. Ballhausen: Mat. Fys. Medd. Dan. Vid. Selsk. **33**, no. 5 (1961).
8. — — Advances quantum Chem. **4**, 170 (1967).
9. Holt, S. L., and C. J. Ballhausen: Theoret. chim. Acta (Berl.) **7**, 313 (1967).
10. Huzinaga, S.: J. chem. Physics **36**, 453 (1962).
11. Löwdin, P. O.: J. chem. Physics **21**, 374 (1953).
12. — Philos. Mag. Suppl. Vol. 5, No. 17 (1956).
13. Mulliken, R. S.: J. Chim. physique **46**, 497, 675 (1949).
14. Oleari, L., G. De Michelis, and L. DiSipio: Molecular Physics **10**, 111 (1966).
15. Palenik, G. J.: Inorg. Chem. **6**, 503 (1967).
16. — Inorg. Chem. **6**, 507 (1967).
17. Palke, W. E., and R. M. Pitzer: J. chem. Physics **46**, 3948 (1967).
18. Pople, J. A., D. P. Santry, and G. A. Segal: J. chem. Physics **43**, S 129 (1965).
19. Ransil, B. J.: Rev. mod. Physics **12**, 245 (1960).
20. Richardson, J. W., W. C. Nieuwpoort, and R. R. Powell: J. chem. Physics **36**, 1057 (1962).
21. —, R. R. Powell, and W. C. Nieuwpoort: J. chem. Physics **38**, 796 (1963).
22. Roothaan, C. C. J.: Rev. mod. Physics **23**, 69 (1951).
23. Watson, R. E.: Physic. Rev. **119**, 1934 (1960).
24. Wyckoff, R. W. G.: Crystal structures, Vol. 3. Second Edition. New York: Interscience Publishers 1965.

Dr. J. P. Dahl
Department of Physical Chemistry
The University of Copenhagen
Universitetsparken 5
Copenhagen/Denmark